The Journal of Young Investigators
The premier undergraduate research journal

Mitigation through the Use of a Near-Shore Undersea Trench: A Physical and Mathematical Model

Julia Benson

Deerfield High School
Deerfield, Illinois, 60015

Volume 20, Issue 3
September 2010

Mitigation through the Use of a Near-Shore Undersea Trench: A Physical and Mathematical Model

Julia Benson
Deerfield High School, Deerfield, Illinois, 60015
jhbenson27@aol.com

ABSTRACT

Purpose: Although the 2004 Indian Ocean tsunami was the most devastating in history, tsunamis are a recurring peril for all coastal communities. This experiment evaluated the possibility of using an undersea trench, offset from the shore, to physically reduce wave amplitude at the shoreline.
Procedures: A wave tank of 4.7 x 1 with a depth of 1 meter was utilized. 30 models were created using three different trench depths and widths in all combinations for each of three sea floor slopes along with a control that had no trench. Fives waves were generated for each configuration and wave amplitude was measured at the leading edge of the shoreline. Video frame analysis was used to assess waveform. A 3-way factorial analysis evaluated the effects of the three independent variables using SAS. The LaGrange's Interpolation Formula created a polynomial relating the variables to wave amplitude.
Data: Both trench depth and width independently resulted in statistically significant reductions in wave amplitude. While wave height increased with decreasing slopes, trench benefit increased. Model waveform and Froude number were quite similar to the 2004 tsunami.
Conclusion: The largest trench, with the shallowest slope, reduced wave amplitude by 53% and the estimated energy transfer to land by 77%. Given the dynamic and geometric similarities with tsunamis, this experiment suggests wave mitigation may also be seen at larger scales. Operating continuously and passively, a near-shore trench might be a valuable supplement to early warning and evacuation. Further evaluation of this concept using shallower slopes may have merit.

INTRODUCTION

On December 26, 2004 at 00:58:53 GMT, a magnitude 9.2 earthquake occurred off the coast of Sumatra in the Indian Ocean [Lay *et al*., 2005]. The earthquake generated a tsunami that killed roughly 227,000 people with at least 70,000 more people missing and presumed dead [*Stewart*, 2005]. No coastal area is immune. In the decade 1990 to 1999, 82 tsunamis caused 4,600 deaths and more than $1 billion in damages [*IOC*, 2008]. More recently, on July 17, 2006, another tsunami struck Java, on the southern coast, killing an estimated 730 people [*Lavigne et al*., 2007]. Recent threats posed by tsunamis provide strong incentive to further mitigation efforts and coastal protection.

Current work focuses on the practice of early warning and vertical evacuation. Tsunami prediction efforts are exemplified by the placement of seismic sensing buoys in the Pacific Ocean via the Deep-ocean Assessment and Reporting of Tsunamis system (DART™) [*NOAA: DART*™, 2007]. The actual prediction process is performed by specifically developed software "Methods of Splitting Tsunamis" (MOST) [*NOAA: Tsunami Modeling and Research*, 2007]. Public warnings are issued by the Pacific Tsunami Warning Center (PTWC). Yet, despite significant advances in tsunami early warning, a central aspect of near-shore seismic events is that they often leave little time for evacuation. The 2009 tsunami that struck Samoa arose from an earthquake 250 kilometers off the coast but arrived only 20 minutes after the quake [*Associated Press*, 2009]. In view of the little time that near-shore earthquakes allow for evacuation, recent tsunami mitigation efforts have focused on vertical evacuation [*FEMA*, 2008] [*Heintz and Robertson*, 2008] [*Heller*, 2005]. This idea is practical and emphasizes movement upward rather than the more time consuming inshore evacuation. However, there are no empirical observations of the actual

stresses that tsunamis place on shoreline structures at the present [*Charvet*, 2009].

Physical tsunami mitigation efforts have also been implemented, but they have made little impact on lessening tsunami damage and can bar easy access to the ocean. In some coastal areas of Japan, walls 4.5 meters high have been built to redirect the water in the event of a tsunami. Mangrove trees have also been planted for the same reason ["Tsunami: Magnitude of Terror", 2005].

Given the current difficulties with protecting coastal communities from tsunamis, the question was asked if additional mitigation approaches might have merit. Specifically, is a mechanism available to reduce tsunami wave amplitude, and thereby, energy transfer to land before the tsunami arrives at the coastline? Given the fact that tsunamis chiefly cause damage when the open ocean wave shoals near the beach, one promising approach would be to interfere with this process. As the wave enters shallow depths, the wavelength and velocity decrease, but the amplitude increases. This experiment was intended to test the hypothesis that an ocean-floor trench near, but not directly at the water-land interface, could disrupt this process. A secondary objective was to characterize the relative importance and interactions of three independent variables on wave amplitude: ocean floor slope, and trench depth and width. Searches in the scientific and engineering literature in 2007, 2008, and 2009 (key words: tsunami mitigation, ditch, trench) were unable to identify any studies of this concept. Secondary searches of published papers were unable, still, to indentify references to wave amplitude reduction with a trench or ditch.

MATERIALS AND METHODS

The experiment was designed to have analyzed variations in sea floor slope, trench depth, and trench width. To increase the chance that effects on wave amplitude would be found, the variations in the independent variables were maximized within the physical limitations of the tank. Trench depths and widths of 40, 60, and 80 centimeters were tested in all combinations along with a control for each slope. The tank length of 4.7 meters limited the shallowest slope to a grade of 28.6%. The other grades to be tested were 33.3% and 40%.

A wooden wave tank was built and placed within a 5.5 x 3 x 1.3 m Intex® above-ground swimming pool containing 12,378 liters of water. The entire experiment was conducted in the basement of a residential home after consultation with a structural engineer (to protect the home). The pool was filled and drained as needed with a 30 meter long, 1.5 centimeter diameter garden hose from the home's exterior water outlet and two 25 kilogram-meter/second 3 centimeter ejection valve sump-pumps. The wave tank walls were 4.7 meters long. The walls where the wave was generated (the side farthest from the beach) were 2 meters high for the first meter, then 1.5 meters high for the next 1.5 meters. The remainder of the wall was 1.28 meters high. The beach wall was one meter high, 50 centimeters wide and comprised of 2 centimeter thick plywood (Figure 1).

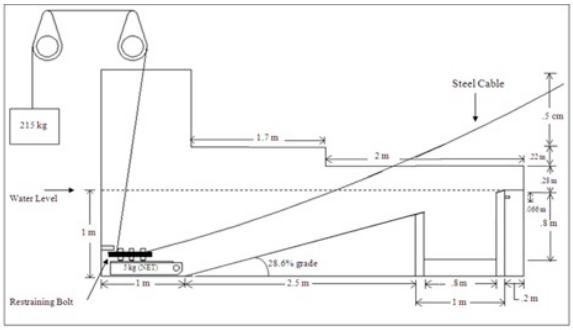

FIGURE 1. This depicts a side-view of the wave tank set-up. The sea floor slope structure was placed directly in front of the trench structure. The structure that served as the beach was located at one end of the wave tank, whereas the wave generator was located at the opposite end, in front of the slope.

A custom slot was cut into the leading edge for placement of the wooden wave gauge. A small piece of wood was screwed to the

inside of the beach support to provide a bottom stop for the wave gauge—a disposable wooden paint stirring stick 36 centimeter long. The walls of the wave tank itself had to be ballasted with forty 22.7-kilogram concrete blocks to prevent them from floating and keep them in place.

The mass drop assembly was a base of 5 x 15 centimeter pine upon which two additional 5 x 15 pieces of pine were screwed with 10-centimeter deck screws. (Figure 2)

FIGURE 2. The mass drop assembly consisted of various weights linked together by chain. The bulk of weights was then attached to a manual chain hoist with a 1 ton lifting capacity. Once the bolt-compression spring mechanism was released from its resting position, the weights were free to fall, generating a wave.

Holes that were 3 centimeter in diameter were drilled at 0.3 meters intervals to accommodate a 907-kilogram load bearing chain. The 454 kilogram capacity snatch blocks and manual chain hoist were hung by chains from this 2 meter beam. The beam rested on a horizontal steel I-beam, 2.4 meters above the ground, which was one of the basement ceiling's exposed, support members for the house. It was further stabilized by four 10 centimeter C-clamps that secured the lip of the wooden beam to the lip of the steel beam at the four corners of their intersection.

The second sub-assembly was the wave generator, which was locked into place and then released via a bolt releasing mechanism. (Figure 3)

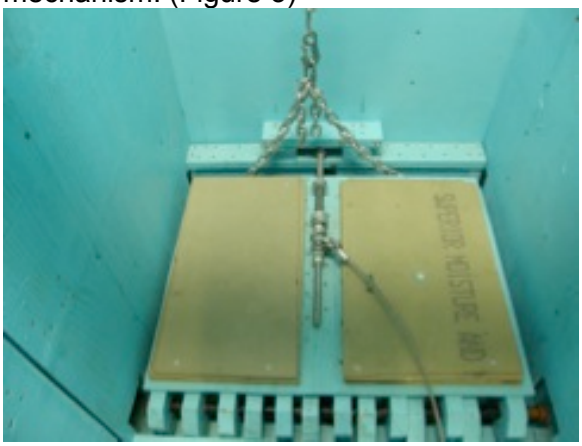

FIGURE 3. A compression spring was placed around a bolt, creating a bolt-compression spring mechanism. This mechanism was secured to the top piece of plywood on the wave generator. Its resting position was under the 2 x 4 plywood. Once the bolt was released from this position, the wave generator would be uplifted, generating a wave.

A steel bolt, 2 centimeters in diameter and 60 centimeters long, was secured to the top end of the wave generator by two 2-centimeter screw-eye bolts with a 7.6 centimeter compression spring sandwiched between two 2 centimeter washers. The 7.6 centimeter long compression spring had an outer diameter of 2.4 centimeters and a load of 40.8 kilograms. The end of the 60-centimeter bolt closed to the opening of the wave generator had a 1 centimeter thick steel cable attached. This mechanism permitted the 60-centimeter bolt to extend beyond the top of the wave generator plank beneath the brass plate secured to the 5 x 10 centimeter stud in the wall at the closed end of the wave generator. The plank itself was ballasted with 40 kilogram of iron plate in sealed plastic bags beneath it. This gave the plank a negative buoyancy of 5 kilogram to assure that it would drop back down to its locking position after the return of the 215-kilogram mass to its starting height. With traction on the steel cable by the manual chain hoist, the bolt was pulled back 2 inches releasing the wave generator plank which was then pulled upward by the steel

cable attached to the mass via a pulley system (Figure 1).

The slopes were 96 centimeters wide to ensure proper fitting within the wave tank walls. For each slope an 80 centimeter x 80 centimeter trench system was made with 10 centimeter lips so that this largest trench was contained in a structure 96 centimeter wide and 1 meter long and one meter deep at the point nearest the beach. A 40-centimeter platform and 20-centimeter platform were created as inserts to permit a 60-centimeter deep trench and a 40-centimeter trench. For each trench depth, two additional inserts were created to permit narrowing the width to 60 centimeters and then 40 centimeters.

For each trial, 215 kilograms of weights were hoisted using a 907-kilogram manual chain hoist suspended from the custom wooden beam resting on the basement I-beam. On the other end of the tank, there was a second chain hoist attached to a 10-millimeter, vinyl coated steel cable, with a 907-kilogram working strength. This cable was connected to a spring-bolt compression system. The bolt extended under a piece of wood in front of the wave generator plank. Once the bolt was "locked" into position, resting under the block of wood, the 215 kilograms of weights were lowered until the bolt was bearing the weight. The 36-centimeter wave gauge was placed into a slot at the front of the beach structure. When the cable attached to the locking bolt was pulled back with the second manual chain hoist, the bolt was released, and the weights dropped, creating an uplift of the wave generator. After the wave passed over the beach slot with the wave gauge in place, the gauge was removed and the highest wet mark on the gauge was measured using a metric ruler. (Figures 4 and 5)

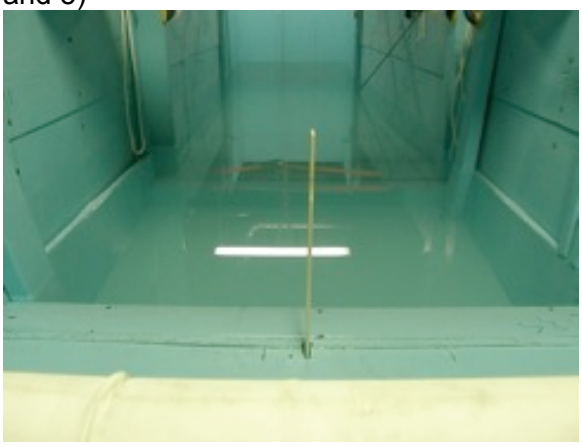

FIGURE 4. This is a rear view of the beach with the wave gauge in place at the front and center of the beach structure. The highest wet mark on the wave measure was recorded. The net was amplitude was calculated by subtracting sea level (the depth that the wave gauge was submerged when placed in the slot) from the highest wet mark after the wave traversed the tank.

FIGURE 5. A wave has been propagated and is now approaching the beach structure. Once the first wave that passes over the wave gauge before reflecting off the back wall of the pool, the wave gauge is pulled out and the highest wet mark is then measured.

The actual water level mark on the gauge with the wave tank at rest was measured five times at the beginning of each day of experimentation to determine "sea level." This averaged value was subtracted from the individual measurements of wave

amplitude to determine the wave's true height above sea level.

A power analysis was used to determine the number of trials for each of the 30 tank configurations required to draw statistically sound conclusions. Ten waves were generated for the 28.6% grade with no trench. Given the small variation in this first series, it was decided to run only 5 waves for the next tank configuration—the 80 x 80 centimeter trench. The power analysis suggested that only one wave per model would discern significant differences. However, it was decided to run 5 waves for each of the 30 tank configurations to increase accuracy and reproducibility. With 5 replicates per scenario, the power analysis indicated that there is over a 99% power for all hypothesis tests (alpha = 0.05).

Data on wave velocity and frequency were obtained by direct observation. Wavelength was both derived from velocity and frequency and roughly confirmed by examination of the video frames analysis. A Sony mini-DVD video camera (Model DCR-DVD403 NTSC) recording at 30 frames per second was used to film a wave for the 28.6% slope with an 80 x 80 centimeter trench and without the trench. The format was converted to a .mov format that was studied one frame at a time with iMovie. A wave gauge with 5-millimeter markings was placed in the center of the beach and wave amplitude for each 1/30th second frame was entered into an Excel spreadsheet for both trench and no trench configurations. Water level decrease below initial sea level was roughly estimated at 5 millimeters for both waves as there were no wave gauges placed in front of the beach. Please note that this methodology was different from measuring peak amplitude for the 150 trials that simply measured the highest wet mark on a fresh, unmarked wave gauge for each wave.

The means for each of the 30 configurations were calculated by subtracting the averaged sea level elevation measurement from the averaged wave amplitude measurement to produce the net wave amplitude. With these means, a 3-way factorial analysis of variance (ANOVA) was used to examine the impact of trench depth and width and sea-floor slope on resulting wave amplitude. Analyses were conducted in SAS v9 (SAS Institute, Inc, Cary, NC). Pilot data were used to estimate the variability in means for the ANOVA. The LaGrange's Interpolation Polynomial was used to formulate an equation that would produce interpolating grids using C++ software.

Equation 1. Lagrange's Interpolating Formula

Equation 2. Lagrange Polynomial

Equation 3. Experiment's Formula

Equation 4. Experimental Parameters as

Defined in the Interpolation Formula

$$f_n(x) = \sum_{i=0}^{n} L_i(x) f(x_i)$$

$$L_i(x) = \prod_{\substack{j=0 \\ j \neq i}}^{n} \frac{x - x_j}{x_i - x_j}$$

$$H(D,W,S) = \sum_{i=0}^{3} \sum_{j=0}^{3} \sum_{k=0}^{2} H(D_i, W_j, S_k) l_{ijk}(D,W,S)$$

$$l_{ijk}(D,W,S) = \prod_{m=0, m \neq i}^{3} \frac{D - D_m}{D_i - D_m} \prod_{n=0, n \neq j}^{3} \frac{W - W_n}{W_j - W_n} \prod_{p=0, p \neq k}^{2} \frac{S - S_p}{S_k - S_p}$$

Lagrange's interpolating formula is given by Equation 1 where n in $f_n(x)$ stands for the n^{th} order polynomial that approximates the function $y = f(x)$ given at $n+1$ data points as $(x_0, y_0), (x_1, y_1), \ldots\ldots, (x_{n-1}, y_{n-1}), (x_n, y_n)$, as in equation 2. For this experiment, the formula is given by equation 3, where:

$l_{ijk}(D_m, W_n, S_p) = 1$ if $m=i$, $n=j$, $p=k$ otherwise 0 and,

$\vec{D} = [0,40,60,80]$

$\vec{W} = [0,40,60,80]$

$\vec{S} = [28.6,33.3,40]$

and all values for D, W, S remain within these ranges (interpolation).

RESULTS

Three features of the model wave are notable through video frame analysis (Figures 6 and 7).

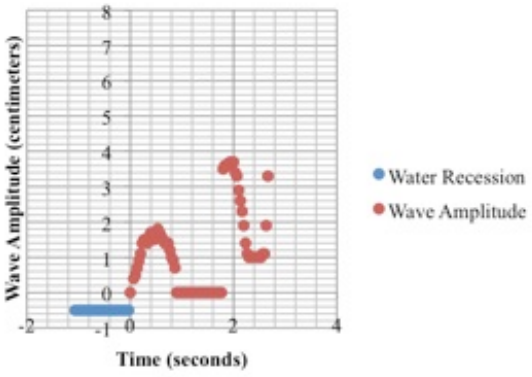

FIGURE 6. Wave Amplitude as a Function of Time (without trench)
The profile of the oncoming wave was filmed using a mini video recorder. Amplitude measurements were taken at every 1/30th of a second. The resulting position graph depicts a wave that has just hit the beach after passing over the sea floor without a trench.

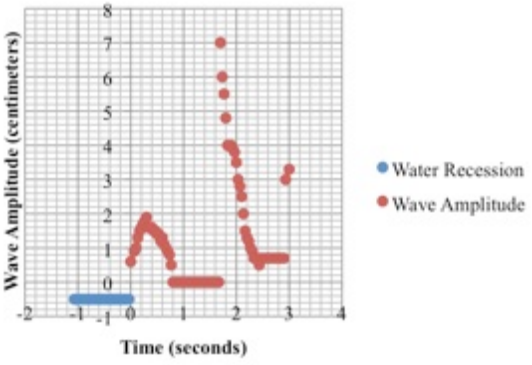

FIGURE 7. Wave Amplitude as a Function of Time (with trench)
The profile of the oncoming wave was filmed using a mini video recorder. Amplitude measurements were taken at every 1/30th of a second. The resulting position graph depicts a wave that has just hit the beach after passing over the sea floor with an 80 x 80 cm trench in place.

Before the initial wave hit the "beach," the water receded. While this was clearly visible from the film, it was difficult to quantify this beyond the start and stop time since the water receded down the slope but there was no fixed measuring stick or point beyond the beach. As a result, the -0.5 centimeter is only a crude approximation but does help show the phenomenon as a function of time. With and without the trench, a small wave is seen before the arrival of the large wave. Following the major wave, sea level remains somewhat elevated for both sea floor configurations, demonstrating a tsunami bore.

Table 1 shows that the 2004 wave amplitude was 333 times higher than the model wave and that its wavelength was 587 times longer, with a velocity six times greater. The Reynolds number for both waves was consistent with the turbulent flow seen in breaking waves although the tsunami wave value was four orders of magnitude higher. The Froude number, more relevant here where gravitational forces predominant (over viscous forces reflected in the Reynolds number), were very similar.

Figures 8-10 depict the average wave amplitude of 5 trials for each of the 30 coastal configurations.

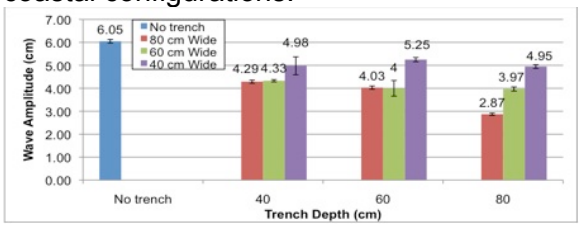

FIGURE 8. Mean Wave Amplitudes for Trench Depth and Width for 28.6% Grade Slope*

* bars = 1 standard deviation
n= 5 trials for each mean (bar)

The means depicted in this graph are the averages of 5 trials ran for each configuration. With the 28.6% grade slope in place, trench depths and widths of 40, 60, and 80 cm were tested in all combinations in addition to the control group of the no trench.

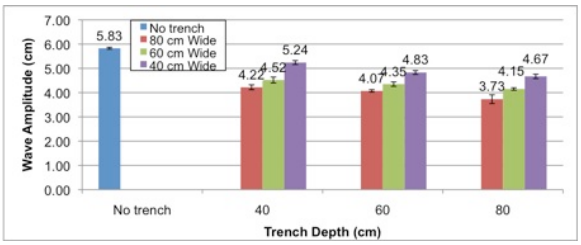

FIGURE 9. Mean Wave Amplitudes for Trench Depth and Width for 33.3% Grade Slope*

* bars = 1 standard deviation
n= 5 trials for each mean (bar)

The same methods were used to collect the mean wave amplitudes for the 10 configurations for the 33.3% grade slope as were used for the 28.6% grade slope.

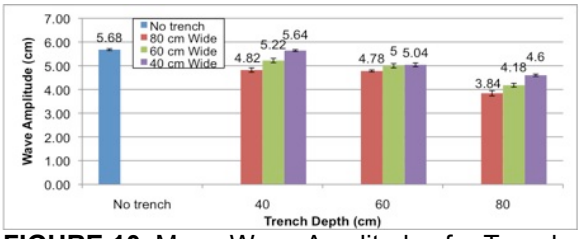

FIGURE 10. Mean Wave Amplitudes for Trench Depth and Width for 40% Grade Slope*

* bars = 1 standard deviation
n= 5 trials for each mean (bar)

The same methods were used to collect the mean wave amplitudes for the 10 configurations for the 40% grade slope as were used for the 28.6% grade and the 33.3% grade slope.

Wave amplitude diminished for each of the trenches in comparison with the control configuration with no trench. The control wave amplitude diminished as the slope became steeper and the reduction in wave amplitude for a given trench size diminished also. The largest trench for the shallowest slope caused a 53% reduction in wave amplitude. Figures 11 and 12 show that that even though tsunami height increased as the slope became shallower, the benefit of a given trench increases on both an absolute and percentage basis.

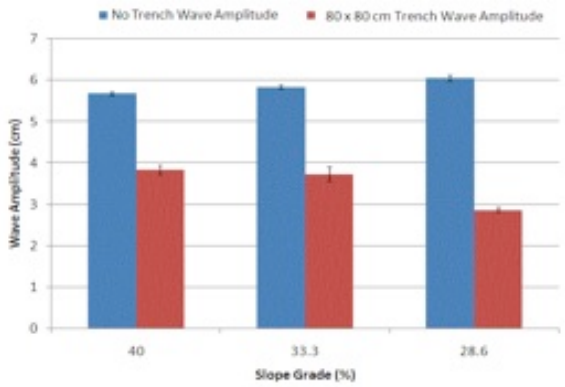

FIGURE 11. Wave Amplitude Reduction as a Result of an 80 x 80 Centimeter Trench

The juxtaposition of the wave amplitude before and after the placement of the 80 x 80 cm trench on the sea floor reveals that the wave amplitude increased as the slope became shallower. However, the benefit of the trench increased as the slope became shallower, yielding the largest reduction and the smallest net wave amplitude for the 28.6% grade slope.

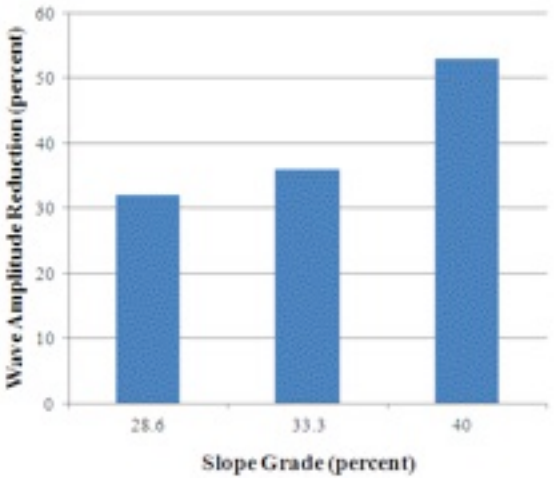

FIGURE 12. Percentage of Wave Amplitude Reduction as a Result of an 80 x 80 Centimeter Trench

The complement of the quotient of the mean wave amplitude that resulted from the implementation of the 80 x 80 cm trench over the mean wave amplitude without the use of a trench yielded the values in the graph. The benefit of the trench drastically increased as the slope grade became shallower.

With five trials per model, most of the differences between means were highly significant—in most cases with p values < 0.0001 as shown for the 28.6% slope. (Table 2, next page) The p-values for the 33% and 40% slopes were very similar.

The three-way analysis of variance (ANOVA) model described in Table 3 (next page) showed that the contribution of each of the three independent variables and their interactions with each other were highly significant. As shown in Table 4 (next page), both depth and width were strongly related to wave amplitude, resulting in improvements in the R^2 value of 60% and 73%, respectively, over a model that does not account for trench characteristics at all. The full model with all interactions offers further improvement, suggesting that both depth and width are jointly important predictors of wave amplitude. Table 5 (next page) is an attempt to define the relative importance of each variable and suggests that the slope itself is the least important variable while trench width may have slightly more impact than depth. The fact that all three variables together accounted for 96% of the variance suggests that there was little impact of uncontrolled influences on wave amplitude.

A mathematical formulation was attempted using the three independent variables together with the empirically determined dependent variable. It was decided to utilize LaGrange's interpolation formula to generate a polynomial rather than more complicated approaches such as the creation of a trigonometric or exponential series.

The actual calculation was performed utilizing C++ programming with the specific wave amplitudes for a given trench depth and width generated in graphic format for each of the three slopes. (Figure 13)

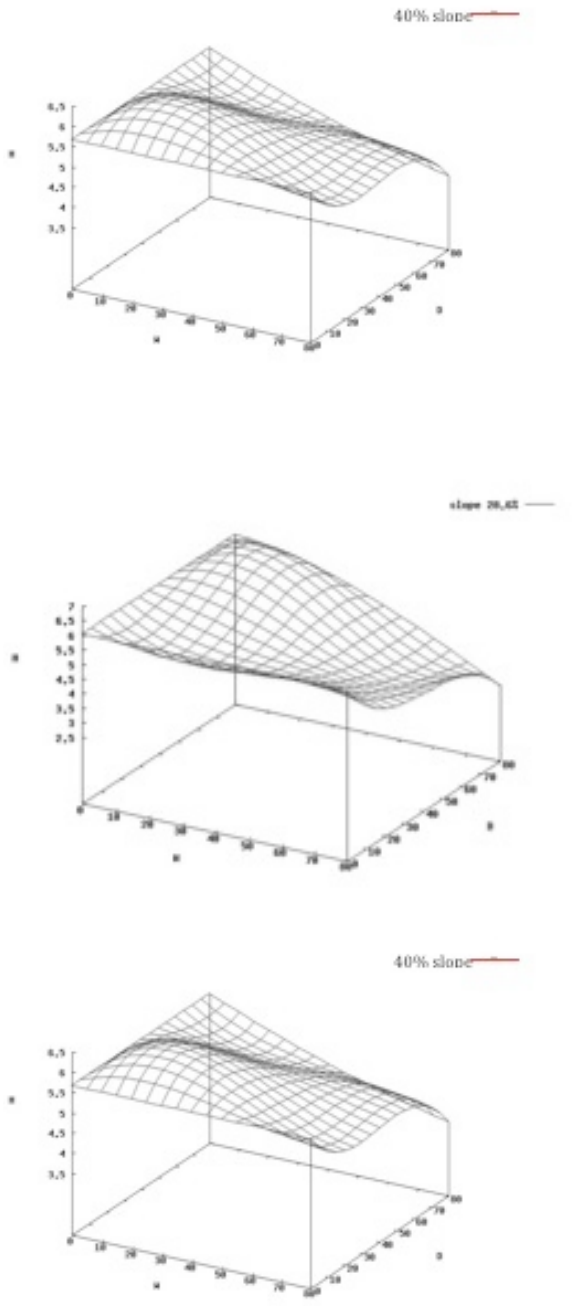

As expected, extrapolation for variable ranges outside the initial experimental parameters was not reliable. For instance, using a trench depth and width of 80 centimeter (within experimental parameters) and slope of 20% (outside of parameters),

the formula predicts a wave amplitude of –2 centimeter, an obviously impossible result.

CONCLUSIONS

The hypothesis that wave amplitude could be reduced through the use of a near-shore undersea trench was proven. The effect was large (up to 53%) and highly statistically significant. The secondary objective of the experiment to examine the roles of three independent variables was also achieved. Both trench depth and width had independent effects on reducing tsunami amplitude. An unexpected result was that trench benefit increased as the ocean floor grade decreased—both as a percentage reduction of wave amplitude and even in absolute terms. This is perhaps the most important finding of the study.

The fact that 96% of the variance in wave amplitude was explained by the three independent variables suggests that there was little influence of confounding or unidentified variables. Potential sources of error or experimental variation such as wood warping, tank wall flexing as the wave passed (clearly visible), measurement inconsistency, or variations in initial energy release or water level were evidently minimized. The precision of the wave generation caused most of the standard deviations for mean wave amplitude to be actually less than the lowest unit of measure used here (<1 millimeter). This was attributed to the experimental design that assured the wave generator plank had exactly the same start and stop point for each wave by using a steel cable rather than rope (which could stretch over time) to connect the weights with the wave generator. Finally, five waves were generated for each model configuration rather than the one trial suggested by the power analysis.

As the energy of a wave is proportional to the square of its amplitude, the benefit of wave height reduction exceeds a 1:1 ratio [*Henderson*, 2007]. The height reduction of 53% reported here for the shallowest slope and the largest trench would decrease energy transfer to land by a calculated 77%. This takes on added importance in assessing trench impact on the reduction of tsunami destructiveness. While the typical wave height at Banda Aceh was 20 meters, the run-up on land far exceeded this initial amplitude and occasionally reached heights of 51 meters above sea level [*Lavigne et al*., 2009].

The energy released by the 2004 tsunami at the earth's surface was estimated to be 1.1×10^{17} joules while the energy utilized in this experiment was 1.48×10^{3} Joules [*U.S. Geological Survey*, 2004]. As the energy in the model was 10^{14} times less energetic that a naturally occurring tsunami, the issue of scaling has to be addressed before any assertions about trench performance can be made in natural conditions. For this experiment, dynamic scaling can be evaluated by the Froude number, which is used in fluid mechanics to compare wave similarity in situations in which gravitational force plays a leading role (as it does here with the wave rising up and over the sloping sea floor). It is noteworthy here that the Froude number for the model and 2004 tsunami were very similar (within a factor of three). The Reynolds number was also calculated here; although as a measure of viscous flow is less important for comparison. Rather the high Reynolds numbers for both waves predicts highly turbulent flow, which was observed.

In a somewhat similar experiment using a 10-meter long wave tank with a 30 centimeter depth, similar Froude numbers were found between the model and the 1771 Meiwa tsunami [*Imamura et al*., 2008]. Significantly, their model's Reynolds number was three orders of magnitude less than the Meiwa tsunami, similar to the model/tsunami discrepancy reported here. The authors pointed out, "it is well known that one cannot match both the Reynolds number and the Froude number in the same scaling experiment." Of further note was the fact that the Froude number for their model tank was less than 1.3 and for the 1771 Meiwa tsunami, the Reynolds number was less than 1—both in close agreement

with the values obtained here. Using their model in which the experimental wave and the tsunami wave had similar Froude numbers, they successfully predicted the distance travelled by sea floor boulders that was observed on the Meiwa coastline. The decision here to rely on the Froude number for dynamic scaling is consistent with the literature on tsunami modeling.

A number of geometric parameters are also similar. The waveforms for both waves share water precision, small preceding waves, and the presence of a bore. Also, the ratio of wavelength to amplitude for the 2004 tsunami of 48, is the same order of magnitude as that of the model wave which is 27. Furthermore, it is assumed that the near-shore wall of the trench should be placed as close to land as possible without interfering with beach recreation—at a water depth that is over the height of a human—or roughly three meters. For the 28.6% slope, the 0.1-meter offset meant that a near-shore wall of the trench started at 0.029 meters. For a 3-meter depth at scale, the trench wall would start at 10.5 meters from the beach.

However, geometric scaling remains limited because the shallowness of coastal seafloor slopes could not be matched due to the physical limitations of the tank used here. In the previously cited work, the authors used a 10-meter tank with 30 cm water depth and were able to achieve a slope of 10%—still quite high for natural coastlines [*Imamura et al*., 2008]. The slope off Hilo, a volcanic island is 8% while off Monterey Bay and New York, is less than 1% [*Google Earth*, 2009] [*Taylor*, 2008] [*Divins*, 2008]. The data here show that for a given energy release, tsunami amplitude is greatly affected by near shore grade and that trench effectiveness is even more influenced. As an aside, the influence of the coastal slope and the increasing energy effects of tsunamis for more shallow slopes were observed for in a 2009 study [*Goto et al*., 2009]. Trench benefits simply could not be extrapolated for slopes less than the 28.6% used here as both tsunami amplitude and trench benefits do not have simple, linear relations with sea-floor slope.

This experiment appears to be the first of its kind to examine the potential of an undersea trench to mitigate tsunami wave amplitude. This study established that: 1) wave amplitude increased with decreasing sea floor slope, 2) increasing trench depth and width each had independent effects on reducing tsunami height, 3) the benefit of the trench increased as the sea floor became shallower, and 4) the trench does not have to be located directly at the sea/land boundary.

A near-shore trench would provide 24/7 passive protection for lives and property, have minimal environmental impact, and permit unrestricted beach access and ship navigation. Given the similarity in waveform and Froude numbers between the experimental model and the 2004 Tsunami, further modeling utilizing waves with shallower sea-floor slopes may have merit. Furthermore, trench effects on a series of waves, common in tsunamis, may also be of interest. Modeling of such a series of low frequency waves is becoming a practical reality with the construction of at least one wave tank specifically built for such a purpose in collaboration between the University College of London and HR Wallingford in Great Britain [*Weston*, 2007].

ACKNOWLEDGMENTS

The author would like to acknowledge the assistance of the following people:

1) Michael D. Benson, MD, Clinical Assistant Professor, Obstetrics and Gynecology, Feinberg School of Medicine, Northwestern University—Experimental design, construction, project safety, funding

2) Jordan Benson—Construction

3) Jennifer Beaumont, MS, Research Statistician, Department of Medical Social Sciences, Feinberg School of Medicine, Northwestern University—statistical analysis

4) Jonathan Remo, PhD., P.G., Research and Project Manager, Department of Geology, Southern Illinois University—geological considerations, citations, and ocean floor data

5) Bruce Burris, CE, MS, consulting civil engineer—waveform considerations, model extrapolation

6) Peter Daut, Atlas Consulting—Video formatting

7) Euginio, Aulisa, PhD. Assistant Professor, Department of Mathematics and Statistics, Texas Tech University—Mathematical Modeling

8) Stephen H. Davis, PhD. Walter P. Murphy Professor Applied Mathematics, McCormick School of Engineering, Northwestern University and Michael Gratton, PhD, Post Doctoral Associate, Applied Mathematics, McCormick School of Engineering, Northwestern University—Scaling considerations

REFERENCES

Associated Press. (2009). 119 Dead, Villages 'Wiped Out' in Samoa Tsunami. Fox News.
Retrieved September 30, 2009, from http://foxnews.com/story/0,2933,557282,00.html.

Charvet I., W. Allsop, T. Lloyd, D. Robinson, T. Robinson, T. Rossetto. (2009) Physical modeling of violent flows and their impact using a new tsunami generator. Earthquake and Tsunami Conference (EQT 2009) Istanbul, Turkey.

Divins, D.L., & Metzger, D. 2008. NGDC Coastal Relief Model, http://www.ngdc.noaa.gov/mgg/coastal/coastal.html. Retrieved January 20, 2009.

FEMA. (2008). Guidelines for Design of Structures for Vertical Evacuation from Tsunamis. FEMA P646 Report, Federal Emergency management Agency, Washington D.C.

Google Earth v5.1. 19°42′20″N 155°5′9″W. Retrieved August 9, 2009.

Goto, K., K. Okada, and Imamura, F. (2009). Importance of the Initial Waveform and Coastal
Profile for Tsunami Transport of Boulders. Polish Journal of Environmental Studies,18 (1), 53-61.

Heintz, J.A., & Robertson, I.N. (2008). Design of Structures for Vertical Evacuation from
Tsunamis. Solutions to Coastal Disasters 2008: Tsunamis, 72-75.

Heller, V., J. Unger, & Hager, W. (2005). Tsunami Run-up—A Hydraulic Perspective. Journal
of Hydraulic Engineering, 743-747.

Henderson, Tom. (2007). Properties of Waves. Retrieved July 2, 2007 from http://www.glenbrook.k12.il.us/gbssci/phys/class/waves/u10l2c.html.

Imamura, F., K. Goto, & Ohkubo, S. (2008). A numerical model for the transport of a boulder
by tsunami. Journal of Geophysical Research, 113, 1-12.

Intergovernmental Oceanographic Commission. 2008. Paris, UNESCO. IOC Technical Series,
85.

Lavigne, F., C. Gomez, M. Giffo, P. Wassmer, C. Hoebreck, D. Mardiatno, J. Prioyono, &
Paris, R. (2007). Field observations of the 17 July 2006 Tsunami in Java. Natural Hazards
and Earth System Sciences,7, 177-183.

Lavigne, F., R. Paris, D. Grancher, P. Wassmer, D. Brunstein, F. Vautier, F. Leone, F. Flohic, B.

De Coster, R. Gunawan, C. Gomez, A. Setiawan, R. Cahyadi, & Fachrizal. (2009). Reconstruction of tsunami Inland Propagation on December 26, 2004 in Banda Aceh, Indonesia, through Field Investigations. Pure Applied Geophysics, 166, 259-281.

Lay, T., H. Kanamori, C. J. Ammon, M. Nettles, R. Aster, S. L. Beck, S. Bilek, M. R. Brudzinski,
R. Butler, H. R. DeShon, G. Ekström, K. Satake, S. Sipkin, S. & Ward, N. (2005). The
Great Sumatra-Andaman Earthquake of December 26, 2004, Science, 308. 1127–1133.

National Oceanic and Atmospheric Association. (2007). DART™ (Deep-ocean Assessment and
Reporting of Tsunamis) In *NOAA Center for Tsunami Reasearch*. Retrieved June 29, 2007, from
http://nctr.pmel.noaa.gov/Dart/about-dart.html.

National Oceanic and Atmospheric Association. (2007). Tsunami Modeling and Research. In
NOAA Center for Tsunami Reasearch. Retrieved July 3, 2007, from
http://nctr.pmel.noaa.gov/model.html.

Stewart, G.B. (2005). Catastrophe in Southern Asia: The Tsunami of 2004, Thomson Gale,
Detroit.

Taylor, L.A., B.W. Eakins, K.S. Carignan, R.R. Warnken, D.C. Schoolcraft, & Sharman, G.F.
(2008). Digital Elevation Model of Port San Luis, California: Procedures, Data Sources and Analysis. National Geophysical Data Center Marine Geology and Geophysics.

University of Southern California Tsunami Research Center. (2005). 1946 Aleutian Tsunami.
Retrieved April 10, 2009, from http://www.usc.edu/dept/tsunamis/alaska/1946/
webpages/index.html.

U.S. Geological Survey. (2004). USGS Energy and Broadband Solution: Off Western
Coast of Northern Sumatra. Retrieved August 17, 2009, from http://neic.usgs.gov.
Weston, D. (2007). Making waves: How UCL research could minimize the impact of future tsunami. Retrieved July 20, 2009, from
http://www.eurekalert.org/pub_releases/2007-07/ucl-mwh062907.php.